# The Influence of Cocations H, Na, and Ba on the Properties of Cu−Faujasite for the Selective Catalytic Reduction of NO by $NH_3$: An *Operando* DRIFT Study

**Bernard Coq,* Gérard Delahay, Robert Durand, Dorothée Berthomieu, and Enrique Ayala-Villagomez**

*Laboratoire de Matériaux Catalytiques et Catalyse en Chimie Organique, UMR 5618 ENSCM-CNRS, Institut Charles Gerhardt FR 1878, 8, Rue de l'Ecole Normale, 34296 Montpellier, France*

*Received: April 15, 2004*

The selective catalytic reduction (SCR) of NO by $NH_3$ in the presence of $O_2$ has been studied by *operando* DRIFT spectroscopy on four Cu-faujasite catalysts, Cu(0.12)Na−FAU, Cu(0.14)H−FAU, Cu(0.16)Ba−FAU, and Cu(0.38)Na−FAU. From steady-state SCR activity at 523, 623, and 723 K with $NO/NH_3/O_2/He$ (0.2/0.2/3.0/96.6, v/v), the feed was switched to $NO/O_2/He$ (0.2/3.0/96.8), and after stabilization to $NO/NH_3/He$ (0.2/0.2/99.6). The aim was to simulate the SCR catalytic cycle, which obeys a redox couple $Cu^+/Cu^{2+}$. The changes of the Cu oxidation state were identified by following an IR band near 900 $cm^{-1}$, assigned to an internal vibration of $[Cu-O-Cu]^{2+}$, or to a modification of adjacent T−O−T framework vibrations induced by $[Cu-O-Cu]^{2+}$. At the steady state of the SCR at 523 K, there is no band visible near 900 $cm^{-1}$ providing evidence that $[Cu-O-Cu]^{2+}$ is reduced as $Cu^+$. Moreover, the redox cycle with $NO+O_2$ and $NO+NH_3$ shows that the oxidation of $Cu^+$ to $[Cu-O-Cu]^{2+}$ by $NO+O_2$ takes much longer than the reduction of $[Cu-O-Cu]^{2+}$ by $NO+NH_3$ at this temperature. These experiments demonstrate that the oxidation is the rate-determining step when the SCR is carried out at low temperature. At 723 K, DRIFT examinations of the SCR at steady state shows that the catalysts are mainly composed of Cu oxo species, for example, $[Cu-O-Cu]^{2+}$ with the band near 900 $cm^{-1}$. On the other hand, the redox cycle with $NO+O_2$ and $NO+NH_3$ indicates that the oxidation became much faster than reduction. Therefore, and in contrast with the reaction at 523 K, the reduction of $Cu^{2+}$ to $Cu^+$ is the rate-determining step in the SCR at 723 K. The study of the redox properties of the various Cu−FAU catalysts by $NO+O_2$ and $NO+NH_3$ demonstrates that the high activity at low temperature of Cu(0.38)Na−FAU and Cu(0.16)Ba−FAU can be mainly described in terms of a fine-tuning of Cu redox properties.

## Introduction

The selective catalytic reduction by $NH_3$, or urea, (SCR) is the best available control technology for reducing $NO_x$ emissions from stationary sources.[1] Besides the very popular $V_2O_5-TiO_2$ catalyst, zeolite-based materials attract more and more attention.[2−4] They offer high efficiency and selectivity to $N_2$ from low- to high-temperature operations and less disposal issues for spent catalysts. In this class of materials, the most efficient catalysts are transition-metal ions in zeolites (TMI-zeolite).[4] $DeNO_x$ on TMI-zeolite is regulated by the TMI redox couple, for example, $Cu^+/Cu^{2+}$ or $Fe^{2+}/Fe^{3+}$, though the exact nature of these cationic species remains a matter of discussion. Cu−FAU belongs to the most attractive formulations, and the activity reaches a maximum value near full exchange degree in Cu.[5]

Moreover, the nature of the cocation, H, Na, Ba, La, ..., has a definite great influence on the catalytic behavior, and the light-off temperature (50% NO conversion) can be lowered by ca. 150 K depending on the nature and amount of the cocation.[6,7] It was proposed that the most active Cu species are those located in supercage.[5] In this regard, the siting of Cu in supercages is favored by (i) a high Cu content;[5] (ii) the preexchange of FAU with dedicated cations such as Ca, Ba, or lanthanides;[6,8] and (iii) protons as cocations, which make the migration of Cu from hindered positions inside the sodalite cages to supercages easier under reaction conditions.[7] It was also proposed that dinuclear oxocations $[Cu-O-Cu]^{2+}$ within the supercage are the most active species.[5] The role of cocations seems to be not only limited to determine siting and mobility of Cu ions, but the cocation could also have some influence on their redox properties. A faster rate of the oxidation step was thus postulated for CuH−FAU in comparison with CuNa−FAU.[7] Quantum chemical calculations on model clusters provided evidence of a higher lability of $H^+$ in the absence of $Na^+$; the proton would then be captured by oxygen more easily in the oxidation step, $Cu^+ \rightarrow Cu^{2+}$, to yield $H_2O$.[7]

The goal of the present work was therefore to investigate the influence of cocations on CuH−, CuNa−, and CuBa−FAU on the redox properties of Cu species. This study was carried out by studying redox cycles with $NO+O_2$ and then $NO+NH_3$ under diffuse reflectance IR examination (DRIFT) at various temperatures. We showed that the mixture $NO+O_2$ oxidizes $Cu^+$ to $Cu^{2+}$, and then $Cu^{2+}$ is easily reduced by $NO+NH_3$.[5]

## Experimental Section

**Preparation of the Catalysts**. The Cu−FAU samples prepared for this study were labeled as follows: Cu(*x*)Na,H,-Ba−FAU, *x* being the Cu/Al molar ratio. The starting zeolite was Na−FAU (Süd Chëmie, Si/Al ≈ 2.55, $S_{BET} \approx 700\ m^2\ g^{-1}$). Details were given previously for the preparation of H−FAU[7]

* Corresponding author. Phone: +33 4 67 16 34 82; fax: +33 4 67 16 34 70; e-mail: coq@cit.enscm.fr.

10.1021/jp040291o CCC: $27.50 
Published on Web 06/30/2004

**TABLE 1: Chemical Composition and Average Number of Al, Cu, Ba, Na, and H[a] Per Unit Cell of the Various Samples**

| | chemical composition (wt %) | | | | | number of atoms per unit cell | | | | | |
|---|---|---|---|---|---|---|---|---|---|---|---|
| sample | Si | Al | Cu | Ba | Na | Al | Cu | Na | Ba | H | Cu/Al (mol/mol) |
| Cu(0.14)H−F AU | 22.0 | 9.0 | 2.90 | | 0.16 | 57 | 8.1 | 0.8 | 0 | 40 | 0.14 |
| Cu(0.12)Na−FAU | 22.0 | 8.80 | 2.50 | | 5.90 | 56 | 6.7 | 42.6 | 0 | 0 | 0.12 |
| Cu(0.38)Na−FAU | 22.2 | 8.10 | 7.24 | | 1.97 | 53 | 20.1 | 12.8 | 0 | 0 | 0.38 |
| Cu(0.16)Ba−FAU | 20.6 | 8.10 | 3.0 | 11.0 | 0.66 | 55 | 8.8 | 5.3 | 14.7 | 2.7 | 0.16 |

[a] The number of protons was calculated as H = Al−2Cu−2Ba−Na.

and Ba−FAU[6] from Na−FAU. The catalysts were prepared by pouring 2 g of Na−, H−, or Ba−FAU into the desired amount of a $Cu(NO_3)_2$ solution (≈0.01 mol $dm^{-3}$, pH = 5) and stirring for 24 h at 298 K. The solid was then separated from the liquid phase by centrifugation, washed with deionized water (30 $cm^3$), and centrifugation again. The samples were dried for 1 h in an oven at 353 K, and then calcined overnight at 723 K in nitrogen (60 $cm^3$ $min^{-1}$). The chemical analyses were performed using plasma atomic absorption spectroscopy at the Service Central d'Analyse du CNRS (Vernaison, France).

Detailed characterizations can be found in previous works,[5−7] and chemical compositions are given in Table 1.

**Catalytic Tests and Redox Cycle**. The SCR of NO with $NH_3$ and the redox cycle with NO+$O_2$ and then NO+$NH_3$ were followed by *operando* DRIFT spectroscopy with a Bruker IFS 55 spectrometer equipped with a Spectratech collector and a reacting cell P/N 19930. Catalyst aliquots (≈15 mg) were activated in situ at 723 K in $O_2$/He (5/95 vol/vol, ramp = 10 K $min^{-1}$, flow = 50 $cm^{-3}$ $min^{-1}$) and cooled to reaction temperature. The reaction gas for the SCR (2000 ppm NO, 2000 ppm $NH_3$, 3% $O_2$, balance with He) was fed to the catalyst, at space velocity of 120 000 $h^{-1}$. In these conditions, the NO conversion to $N_2$ is larger than 50% above 523 K.[5−7]

**Quantum Chemical Calculations**. Quantum chemical calculations were carried out on model Cu-faujasite clusters to get additional insights on CuOCu species. Optimization of geometry was performed using molecular and quantum mechanics. The cluster was cut into a solid structure of Na−FAU optimized from molecular mechanics energy minimization[9] and the dangling bonds were saturated with H atoms. We have chosen a cluster composed of cationic sites in the supercage, sites II and III. Two Al distributions were chosen to represent the zeolite and we replaced $2Na^{I}$ in the six-membered ring with $Cu^{II}$. The other $Cu^{II}$ was connected to the other Al atom. A partial geometry optimization relative to the CuOCu oxocation was performed using B3LYP functional. Geometry and energy were converged to within 0.001 Å and 0.1 kcal $mol^{-1}$, respectively.

The extended Wachters basis set (8s6p3d) was used for copper and a standard 6-31G(d) basis for the other elements. The calculations were carried out with the Gaussian(R) 03 program.[10]

## Results and Discussions

**Calcination of the Starting Materials.** Figure 1 shows the spectra of the materials after calcination at 723 K. The main band at ca. 1270 $cm^{-1}$ comes from the specular reflection of the samples. Depending on the Cu content and the nature of the cocations, H, Na, or Ba, the hydroxyl acid bands near 3600 $cm^{-1}$ look more or less intense. The feature which will attract great attention later on is the band appearing in the range 910−890 $cm^{-1}$ (near 900 $cm^{-1}$ in the following). This band was absent on the Na−FAU starting material (Figure 1, trace a). The occurrence of the specular reflection is inevitable because it is impossible to dilute the sample for the SCR reactivity experiments. Because the dilutent may hide some framework

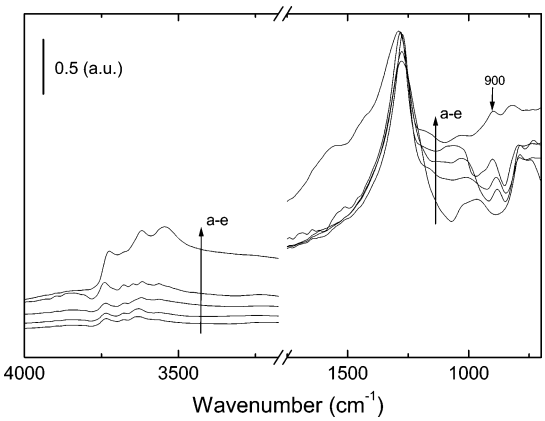


**Figure 1.** DRIFT spectra of the samples after calcination at 723 K; (a) Na−FAU, (b) Cu(0.12)Na−FAU, (c) Cu(0.16)Ba−FAU, (d) Cu(0.38)Na−FAU, (e) Cu(0.14)H−FAU.

vibrations of the zeolite in the region 1250−950 $cm^{-1}$, DRIFT examination in $O_2$/He of Cu(0.38)Na−FAU diluted in KBr (30/70) was carried out. In these conditions, besides the band near 900 $cm^{-1}$, the expected framework vibrations of faujasite were found at 1025 with a shoulder at 1140 $cm^{-1}$.[11] We can therefore unambiguously assign the band appearing near 900 $cm^{-1}$ to a contribution resulting from the calcination of some Cu(II) species. On a 80% Cu-exchanged Na−FAU (Si/Al = 2.5), Valyon and Hall[12] reported a similar band at 909 $cm^{-1}$, which suffered a red shift of 15 $cm^{-1}$ following exchange with $^{18}O_2$. On the basis of the work of Dalla Betta et al.[13] on Fe−FAU, they proposed the antisymmetric stretching mode of Cu−O−Cu to be responsible for this band. However, because of the difficulty to fit this vibration with a model, they postulated that this Cu−O−Cu species may belong to some more complicated structure. The band observed at 932 $cm^{-1}$ upon treating Cu−ZSM-5 in NO+$O_2$ was attributed to a similar species, but bearing an adsorbed oxygen Cu−O−Cu($O_{ads}$).[14] The formation of $[Cu-O-Cu]^{2+}$ in zeolite has been early proposed by Naccache and Ben Taarit[15] from the reaction $2Cu(OH)^{+} \leftrightarrow [Cu-O-Cu]^{2+}$. At low temperature, the reversible hydroxylation/dehydroxylation reaction may occur with a band at 3678 $cm^{-1}$, assigned to the Cu-bound OH group.[12] This reaction is also favored with neighboring $Cu(OH)^{+}$ species,[12] which could tentatively be featured as $[(OH)Cu \square Cu(OH)]^{2+}$. Another explanation was proposed for the occurrence of a band near 900 $cm^{-1}$. The presence of bare, or oxygen-bridged, divalent metal ions (Cu, Co, Ni, ...) at the cationic sites of the dehydrated zeolite would cause local perturbations of the adjacent T−O−T framework vibration (at ca. 1025 $cm^{-1}$ in faujasite) which shifted to lower frequency, that is, 915−910 $cm^{-1}$ in ferrierite and ZSM-5.[16,17] Reduction of divalent to monovalent cations would shift the band to 965 $cm^{-1}$.[16] In Fe-ferrierite, the framework band at 1070 $cm^{-1}$ was shifted to 915 $cm^{-1}$ in the presence of bare Fe(II) cations. Upon interaction of Fe(II)-ferrierite with $O_2$ or $N_2O$, the band then shifted to 880 $cm^{-1}$ because of the formation of a so-called "Fe(III)-O" species.[18]

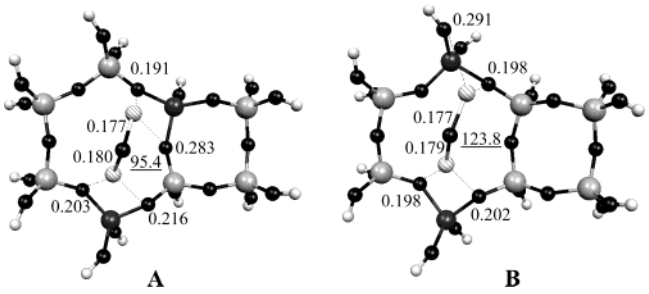


**Figure 2.** Model clusters of CuOCu−FAU; circles denoting Cu, Si, Al are solid crosshatched, gray and black, respectively; smallest circles denoting H and O are solid gray and black, respectively. Bond lengths correspond to Cu−O and are in nm and CuOCu angle values are underlined and in deg.

The TPD in He of the calcined Cu−FAU allowed us to differentiate bare Cu cations from $[Cu-O-Cu]^{2+}$ species, the latter decomposing to $Cu^{+}$ and $O_2$ by treatment at high temperature in Ar or He, whereas bare $Cu^{2+}$ cations were not affected.[19,20] We have thus treated the calcined Cu(0.38)Na−FAU in He at 723 K and the band near 900 $cm^{-1}$ then disappeared, which confirms the origin of this band. However, approximately 90% of the initial $Cu^{2+}$ species remained at the same oxidation state as temperature-programmed reduction (TPR) had shown.[19]

Preliminary quantum chemical calculations on idealized CuOCu−FAU clusters have been then carried out for modeling a better description of this potential active species. Previous theoretical studies by Goodman et al.[21] about CuOCu oxocations in model ZSM-5 clusters were used as a starting basis for our work. They showed that the most stable oxocation structure corresponds to a bent CuOCu with a triplet-state electronic configuration. In fact, this triplet state corresponds to the most stable electronic structure when the CuOCu is bent whereas a singlet-state electronic structure would have been the most stable state for a linear CuOCu. Kieger et al.[5] suggested that the two Cu atoms involved in CuOCu would be located at site II and III of FAU, that is, along the central axes of the six- and four-membered ring, respectively. Actually, during the calculations, such a model cluster CuOCu−FAU disrupts into Cu at site III and CuO at site II. The distance of near 0.4 nm separating site II and III is indeed too long to accommodate CuOCu, for which CuCu distances of 0.291 and 0.313 nm have been experimentally determined from EXAFS of CuOCu−ZSM-5.[22,23]

In contrast, the modeled oxocations with the two copper atoms located above the six-membered containing two Al atoms in different distributions were close to the experimental data (Figure 2). Geometry optimization of the model cluster A, that is, containing the two Al separated by one Si, showed that the oxocation exhibits a Cu−Cu distance of 0.264 nm, in the same range as the 0.248 nm value calculated in CuOCu−ZSM-5[24] and close to the 0.291 nm experimental value.[22,23] The model cluster B, that is, containing the two Al separated by two Si, showed that the oxocation had a Cu−Cu distance of 0.313 nm, similar to the 0.313 nm experimental value mentioned above. Our modeling showed that the bonding of copper to the $O_{oxo}$ is preferred to the $O_{framework}$. In both A and B models, the Cu rised above the ring plane with a preferred Cu−O−Cu bent angle of 95.4 and 123.8 deg, respectively. In these complexes, the Cu net charges (from Mulliken analysis) were far from +2. They were +0.67 and +0.61 in model A and +0.77 and +0.80 in model B, the higher copper charges in model B coming most probably from less bonded oxocations since it has the largest Cu−Cu distance. As already observed in $Cu^{2+}$-exchanged faujasite,[25,26] the spin density analysis illustrates that there is also a charge transfer from the zeolite to copper. Indeed, the spin density on copper is 0.485 and 0.336 in model A and 0.585 and 0.440 in model B, which would be responsible for the EPR signal. These quantum chemical modelings provide evidence that CuOCu may exist as a species in the supercage lying above the six-membered ring connecting the sodalite cavities.

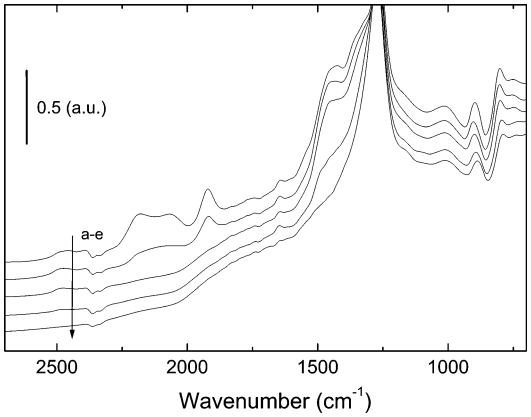


**Figure 3.** DRIFT spectra of Cu(0.16)Ba−FAU interacting with $NO+O_2$ in He (0.02/3/96.8, vol/vol) from 323 to 723 K (ramp: 10 K $min^{-1}$); (a) 323 K, (b) 423 K, (c) 523 K, (d) 623 K, (e) 723 K.

In the following *operando* DRIFT experiments, we will use the band near 900 $cm^{-1}$ as a sensitive probe of the redox catalytic cycle involving the active $[Cu-O-Cu]^{2+}$ species.

**Treatment in $NO+O_2$.** The samples were treated from room temperature to 723 K and the IR spectra recorded every 50 K (see Figure 3 as an example for Cu(0.16)Ba−FAU). The main changes in comparison with the spectra of calcined materials occur in the spectral domains 2200−1800 $cm^{-1}$ (NO region) and 1600−1300 $cm^{-1}$ (nitrate and nitrite region). In contrast, the $[Cu-O-Cu]^{2+}$ species band remains unchanged.

The bands appearing in the spectral domain 2000−1800 $cm^{-1}$ can be assigned to nitrosyl on Cu sites.[27,28] There is no band at ca. 1815 $cm^{-1}$ which could correspond to $Cu^{+}-NO$, and all the bands between 1950 and 1890 $cm^{-1}$ come from $Cu^{2+}-NO$. In comparison with other Cu-zeolite, and specially Cu−ZSM-5, the broad band centered at 1920 $cm^{-1}$ on Cu(0.16)Ba−FAU and the great number of bands on the other samples provide evidence for the variety of $Cu^{2+}$ environment in Cu−FAU. The two unresolved bands at 2180 and 2065 $cm^{-1}$ could tentatively be assigned to nitrosonium $NO^{+}$ ions in interaction with Cu ($Cu^{+}-NO^{+}$) or at cationic positions.[27] All these bands between 2200 and 1800 $cm^{-1}$ follow the same evolution upon heating and vanish above 523 K. These species will not be discussed further.

Two broad IR bands appear on treatment with $NO+O_2$ in the region 1600−1300 $cm^{-1}$ associated with nitro, nitrito, and nitrato species.[27] These bands are more intense with Cu(0.12)-Na−FAU and Cu(0.16)Ba−FAU. However, on the basis of the IR frequencies only it is not possible to interpret these bands.[27] These species desorb, or decompose, above 473 K on Cu(0.12)-Na−FAU and 673 K on Cu(0.16)Ba−FAU.

**Oxidation and Reduction Steps in SCR Reaction.** As reported previously,[5−7] and as shown in Figure 4, the SCR activity as a function of temperature is quite different for the four samples. The *operando* DRIFT examination of the catalyst surface under SCR conditions is exemplified for the sample Cu(0.38)Na−FAU (Figure 5). Several bands appear or vanish in the course of the SCR followed by DRIFT. N−H stretching vibrations of $NH_3$ adsorbed on Cu and Brønsted sites stand in the region 3400−3000 $cm^{-1}$, with progressive disappearance

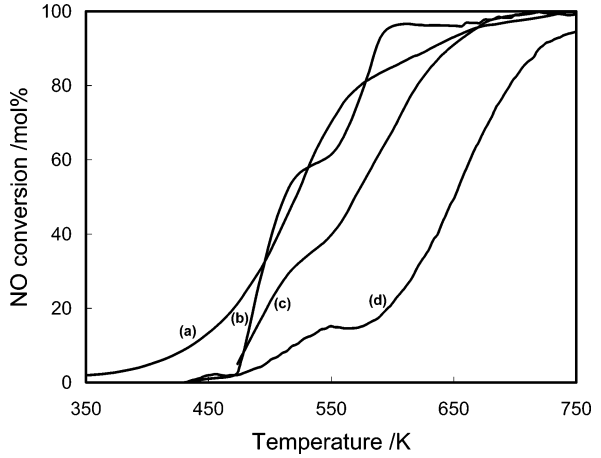


**Figure 4.** SCR of NO by $NH_3$ as a function of temperature on (a) Cu(0.16)Ba−FAU, (b) Cu(0.38)Na−FAU, (c) Cu(0.14)H−FAU, (d) Cu(0.12)Na−FAU. Conditions $NO/NH_3/O_2$/He: 0.2/0.2/3/96.6, ramp = 10 K $min^{-1}$, space velocity: 250 000 $h^{-1}$; data adapted from refs 5−7.

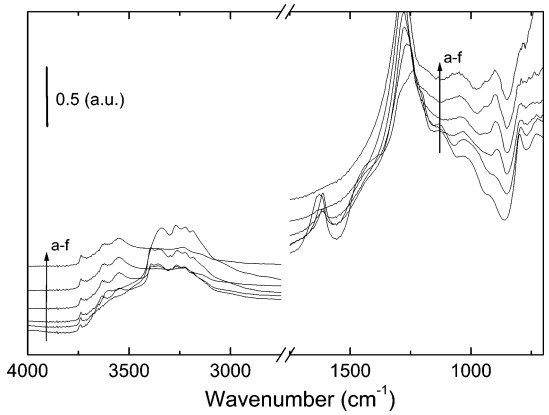


**Figure 5.** DRIFT spectra of Cu(0.38)Na−FAU as a function of temperature during SCR, (a) 373 K, (b) 523 K, (c) 623 K, (d) 643 K, (e) 683 K, (f) 723 K. Conditions $NO/NH_3/O_2$/He: 0.2/0.2/3/96.6, ramp = 10 K $min^{-1}$, space velocity: 120 000 $h^{-1}$.

upon heating above ca. 623−643 K. Bending modes of $H_2O$ and $NH_3$ at ca. 1620−1610 $cm^{-1}$ follow the same trends. The band of $[Cu-O-Cu]^{2+}$ species near 900 $cm^{-1}$ starts to grow significantly above 623 K because of oxidation of Cu in the SCR conditions. The reverse is true at low temperature. Otherwise, we have seen above that the calcined materials contain bare $Cu^{2+}$ and $[Cu-O-Cu]^{2+}$ cations. It was shown that the temperature-programmed treatment by $NO+NH_3$ of calcined Cu−FAU leads to the reduction of $Cu^{II}$ to $Cu^{I}$ associated with $N_2$ evolution centered near 380−390 K.[5,29] The reduction of $[Cu-O-Cu]^{2+}$ species can be regarded as

$$[Cu-O-Cu]^{2+} + 2NO + 2NH_3 \rightarrow 2N_2 + 3H_2O + 2Cu^{+} \quad (1)$$

without generation of proton. In contrast, the reduction of bare $Cu^{2+}$ leads to proton formation:

$$Cu^{2+} + NO + NH_3 \rightarrow N_2 + H_2O + Cu^{+} + H^{+} \quad (2)$$

During the SCR above 643 K on Cu(0.38)Na−FAU, the intensity of bands at 3620 and 3540 $cm^{-1}$ (Figure 5) because of framework Brønsted sites in supercages and sodalite cavities, respectively, remains very low. Since the calcined Cu(0.38)-Na−FAU does not contain proton (Table 1), this feature indicates a low reduction degree of bare $Cu^{2+}$ (the maximum intensity of the generated Brønsted sites according to eq 1 is illustrated by trace *f* in Figure 9). Finally, the very broad shoulder ranging from 1500 to 1380 $cm^{-1}$, which has been tentatively assigned to nitro, nitrito, or nitrato species, vanished above 623 K. The same general tendencies are reproduced with the other catalysts. In particular, the change of intensity of the band near 900 $cm^{-1}$ provides evidence for switching of the Cu oxidation state depending on the SCR temperature.

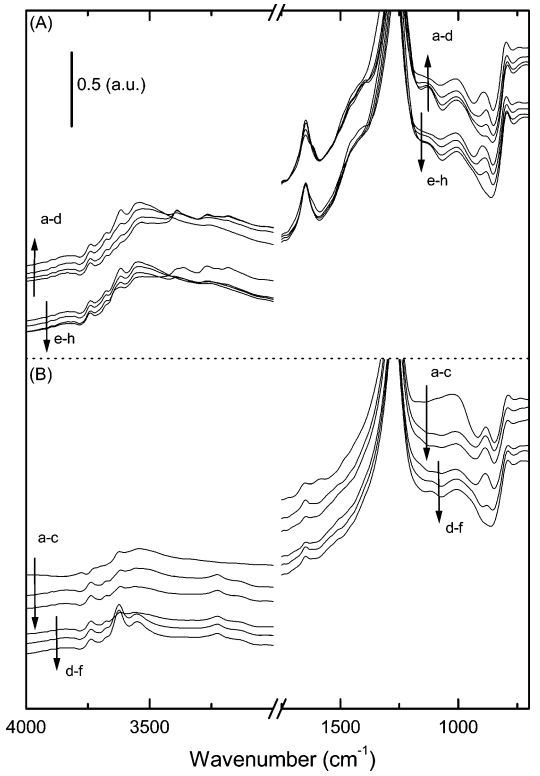


**Figure 6.** DRIFT spectra of Cu(0.16)Ba−FAU as a function of time in redox cycles from steady-state SCR and then to $NO+O_2$ feed and finally to $NO+NH_3$ feed. (A) At 523 K: SCR (a); $NO+O_2$: (b) 10 min, (c) 20 min, (d) 50 min; $NO+NH_3$: (e) 2 min, (f) 5 min, (g) 7 min, (h) 20 min. (B) At 723 K: SCR (a); $NO+O_2$: (b) 5 min, (c) 10 min; $NO+NH_3$: (d) 2 min, (e) 10 min, (f) 15 min.

The SCR on Cu-zeolites is mainly regulated by the $Cu^{+}/Cu^{2+}$ redox couple, and $[Cu-O-Cu]^{2+}$ would constitute the most active species.[5] In this mechanism, $Cu^{+}$ would be oxidized to $[Cu-O-Cu]^{2+}$ by $NO+O_2$, which can in turn be reduced to $Cu^{+}$ by $NO+NH_3$. It has also been suggested that oxidation is the rate-determining step. We examined how the changes in redox properties could explain the catalytic behavior. By *operando* DRIFT, we observed the changes in four samples on going from the steady-state SCR through the redox cycle with $NO+O_2$ and then $NO+NH_3$, and that at three different temperatures. Figures 6−9 present very typical examples of DRIFT spectra of these redox sequences on Cu(0.16)Ba−FAU at 523 and 723 K and Cu(0.14)H−FAU, Cu(0.12)Na−FAU, and Cu(0.38)Na−FAU at 723 K. The hydroxyl and the framework vibration spectral domains were only adressed in these spectra.

The relative intensity of the two bands at ca. 3620 and 3560 $cm^{-1}$ indicates that there are more protons in supercages during the treatment at 723 K by $NO+NH_3$ of Cu(0.12)Na−FAU and Cu(0.16)Ba−FAU. This is in agreement with the TPR experiments on Cu(0.16)Ba−FAU which have shown that the ratio $Cu^{2+}$(supercage)/$Cu^{2+}$(sodalite) was about 3.0.[6] In contrast, TPR experiments on Cu(0.12)Na−FAU demonstrated that $Cu^{2+}$-(supercage)/$Cu^{2+}$(sodalite) was ca. 0.33.[5] This apparent contradiction may indicate that during the treatment of this catalyst

**TABLE 2: Time (in Minutes) for Reaching (i) $(I/I_{max})_{900}$ Value of ca. 0.75 by Switching from the Steady-State SCR to $NO+O_2$ Feed and (ii) $(I/I_{max})_{900}$ Value from 1.0 to 0.25 by Switching from $NO+O_2$ to $NO+NH_3$[a]**

| | switching from SCR to $NO+O_2$ | | | switching from $NO+O_2$ to $NO+NH_3$ | | |
|---|---|---|---|---|---|---|
| sample | 523 K | 623 K | 723 K | 523 K | 623 K | 723 K |
| Cu(0.14)H−F AU | 50 (0.0) | 10 (∼ 0.4) | 0 (∼0.7) | 10 | 7 | 6 |
| Cu(0.12)Na−FAU | 45 (0.0) | 13 (∼ 0.1) | 3 (∼ 0.4) | 6 | 6 | 5 |
| Cu(0.38)Na−FAU | 37 (0.0) | <1 (∼ 0.5) | 0 (∼ 0.9) | 10 | 12 | 19 |
| Cu(0.16)Ba−FAU | 25 (∼0.2) | 0 (∼0.5) | 0 (∼1.0) | 20 | 9 | 8 |

[a] The $(I/I_{max})_{900}$ value at steady-state SCR before switching to $NO+O_2$ is given within brackets.

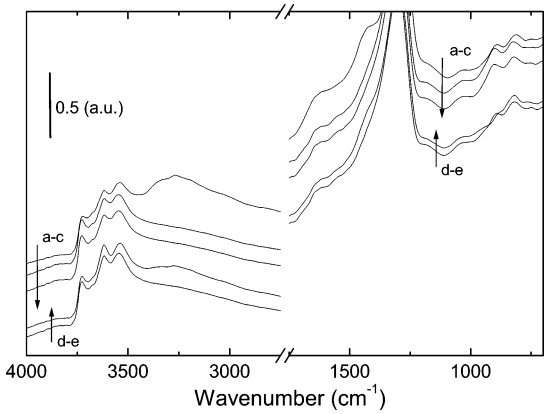


**Figure 7.** DRIFT spectra of Cu(0.14)H−FAU as a function of time in redox cycles at 723 K from steady-state SCR and then to $NO+O_2$ feed and finally to $NO+NH_3$ feed; SCR (a); $NO+O_2$: (b) 10 min, (c) 30 min; $NO+NH_3$: (d) 2 min, (e) 7 min.

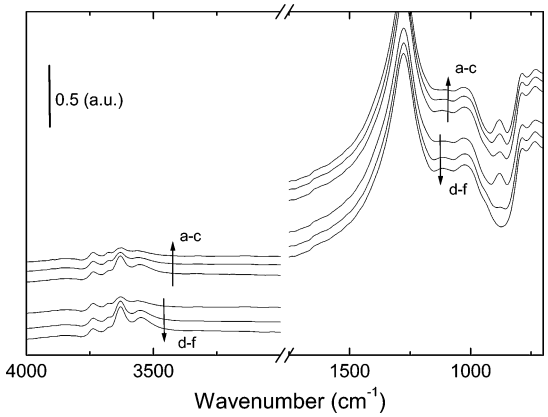


**Figure 8.** DRIFT spectra of Cu(0.12)Na−FAU as a function of time in redox cycles at 723 K from steady-state SCR and then to $NO+O_2$ feed and finally to $NO+NH_3$ feed; SCR (a); $NO+O_2$: (b) 2 min, (c) 7 min; $NO+NH_3$: (d) 2 min, (e) 5 min, (f) 7 min.

at 723 K by $NO+NH_3$ an exchange between $H^+$ (sodalite) and $Na^+$ (supercage) or an ammonia-induced migration of Cu from sodalite to supercage was occurring.

With the aim of comparing the redox properties of the $Cu^+/[Cu-O-Cu]^{2+}$ couple in the various samples, we have estimated the time necessary to reach 75% of the achievement of the forward and backward reaction $2Cu^+ + 1/2O_2 \leftrightarrow [Cu-O-Cu]^{2+}$, upon switching the feed. This was characterized by the relative intensity of the band near 900 $cm^{-1}$ with respect to its maximum intensity reached upon treatment in $NO+O_2$ at 723 K, $(I/I_{max})_{900}$. The values of this parameter have to be considered with care because of (i) the low signal-to-noise ratio in some spectra and (ii) the baseline drift. It is first of interest to look at the value of $(I/I_{max})_{900}$ at the steady-state SCR before switching to $NO+O_2$; the data are given in Table 2. At 723 K, the completion of the $Cu^+$ to $[Cu-O-Cu]^{2+}$ transformation is 100% for Cu(0.38)Na−FAU and Cu(0.16)Ba−FAU but only 40% for

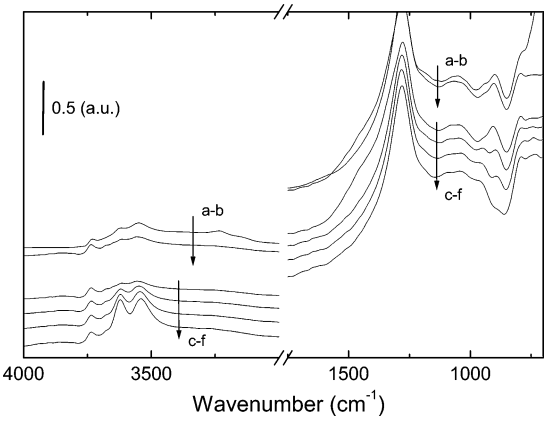


**Figure 9.** DRIFT spectra of Cu(0.38)Na−FAU as a function of time in redox cycles at 723 K from steady-state SCR and then to $NO+O_2$ feed and finally to $NO+NH_3$ feed; SCR (a); $NO+O_2$, (b) 2 min; $NO+NH_3$, (c) 2 min, (d) 10 min, (e) 15 min, (f) 25 min

Cu(0.12)Na−FAU. At 623 K, 50% of $[Cu-O-Cu]^{2+}$ still remains in all samples except Cu(0.12)Na−FAU. Finally, at 523 K $[Cu-O-Cu]^2$ are mainly reduced as $Cu^+$ in all samples, with the remarkable exception of Cu(0.16)Ba−FAU in which 20% of $[Cu-O-Cu]^{2+}$ are still present.

When not already present (vide supra), there is an increase of the band near 900 $cm^{-1}$ upon switching from SCR to $NO+O_2$ feeds. The opposite change then occurs when switching from $NO+O_2$ to $NO+NH_3$. An interesting feature appears when comparing the antagonistic evolutions at 723 K of the band at 900 $cm^{-1}$, because of $[Cu-O-Cu]^{2+}$, and those at 3620 and 3540 $cm^{-1}$, because of framework Brønsted sites. As mentioned above, the reduction of $[Cu-O-Cu]^{2+}$ to $Cu^+$ cannot generate additional protons; then, in the redox sequence from $NO+O_2$ to $NO+NH_3$, other $Cu^{2+}$ species are involved. The reduction of these species to $Cu^+$ thus generates the observed protons. The maximum generation of these protons in the various samples at 773 K is revealed by traces f (Figure 6), e (Figure 7), f (Figure 8), f (Figure 9). If some differences exist at 723 K in the redox couples $[Cu-O-Cu]^{2+}/Cu^+$ and $Cu^{2+}/Cu^+$, they could not be identified in these experiments. We had previously proposed that $[Cu-O-Cu]^{2+}$ would be the most active species in the SCR;[5] the present *operando* DRIFT experiments indeed confirm that $[Cu-O-Cu]^{2+}$, identified by the band near 900 $cm^{-1}$, is very likely involved in the SCR process, but other isolated cationic $Cu^{2+}$ species may also be active. At lower temperatures, 523 and 623 K, it is very difficult to comment about the concurrent evolution of the bands near 900 and 3600 $cm^{-1}$ because of the strong adsorption of $NH_3$ on framework Brønsted sites.

A second point which needs attention is the forward and backward rates of the reaction $2Cu^+ + 1/2O_2 \leftrightarrow [Cu-O-Cu]^{2+}$. These rates were roughly characterized by the time for reaching (i) $(I/I_{max})_{900}$ value of ca. 0.75 by switching from the steady-state SCR to $NO+O_2$ feed and (ii) $(I/I_{max})_{900}$ values from 1.0 to 0.25 by switching from $NO+O_2$ to $NO+NH_3$ (Table 2). Upon

switching from SCR to $NO+O_2$ feeds, at 723 K the transformation of remaining $Cu^+$ to $[Cu-O-Cu]^{2+}$ is immediate for all the samples, except Cu(0.12)Na−FAU for which it stands for 3 min. The amount of $[Cu-O-Cu]^{2+}$ already present at steady-state SCR is the lowest in this sample as the value $(I/I_{max})_{900}$ of 0.4 shows (Table 2). At 623 K, the rate remains fast for Cu(0.38)Na−FAU and Cu(0.16)Ba−FAU but decreases significantly for Cu(0.12)Na−FAU and Cu(0.14)H−FAU. Finally, at 523 K the transformation of $Cu^+$ to $[Cu-O-Cu]^{2+}$, from 25 min for Cu(0.16)Ba−FAU up to 50 min to Cu(0.14)H−FAU, is slow.

Upon switching from $NO+O_2$ to $NO+NH_3$, the reduction of $[Cu-O-Cu]^{2+}$ to $Cu^+$, $(I/I_{max})_{900}$ from 1.0 to 0.25, needs 5−20 min depending on the catalyst and the temperature. It becomes slightly slower when the temperature decreases with the remarkable exception of Cu(0.16)Ba−FAU. These data provide evidence for different behaviors between the samples, which can thus be ranked according to the easiness of oxidability of $Cu^+$ to $[Cu-O-Cu]^{2+}$ as follows: Cu(0.14)H−FAU ≤ Cu(0.12)Na−FAU < Cu(0.38)Na−FAU < Cu(0.16)Ba−FAU. This sequence follows the SCR reactivity order at 523 K (Figure 4). This is an indication that on Cu-zeolite catalysts, oxidation of $Cu^+$ is likely the rate-determining step in the SCR of NO by $NH_3$ at low temperature as hypothesized previously.[5,30−32]

The presence of $NH_3$ ligands on Cu sites could explain in part the difference of $Cu^+$ oxidability between the samples. It seems that to initiate the oxidation of $Cu^+$ in Cu(0.12)Na−FAU at 523 K, it is necessary that 90% of $NH_3$ was desorbed (estimated from the combination bands of $NH_3$ near 5000 $cm^{-1}$). At least one $NH_3$ ligand remains adsorbed on this sample at 523 K, as $NH_3$−TPD experiments have shown.[5] However, $NH_3$ does not inhibit the oxidation of $Cu^+$ in the other samples so strongly. Indeed, 50% $Cu^+$ oxidation was still achieved at 523 K after only 70% $NH_3$ desorption on Cu(0.14)H−FAU and 50% $NH_3$ desorption on Cu(0.38)Na−FAU and Cu(0.16)Ba−FAU. In contrast, the oxidation of $Cu^+$ to $[Cu-O-Cu]^{2+}$ is strongly accelerated upon increasing temperature and the rate-determining step has switched from oxidation to reduction at 723 K.

These *operando* DRIFT studies also allow to understand the remarkable activity of Cu(0.16)Ba−FAU in SCR, despite the low Cu content:

(1) Thanks to the blocking of sodalite cages by Ba, Cu mainly populates the supercages to give rise to the most active Cu species.

(2) Ba accelerates strongly the oxidation of $Cu^+$ to $[Cu-O-Cu]^{2+}$ which becomes as fast as the reduction step even at moderate temperature.

## Conclusions

*Operando* DRIFT experiments during the SCR on Cu−FAU catalysts have put in evidence that

(1) Cu-oxo species, likely of formula $[Cu-O-Cu]^{2+}$, are involved in the redox $Cu^{2+}/Cu^+$ couple which regulates the SCR process. These species, which stand above the six-membered ring separating the supercage from the sodalite cavity, are responsible for an IR band near 900 $cm^{-1}$. This band is due to an internal vibration of $[Cu-O-Cu]^{2+}$ or to modification of adjacent T−O−T framework vibrations. The $[Cu-O-Cu]^{2+}$ is easily reduced by $NO+NH_3$. However, the appearance of protons upon reduction by $NO+NH_3$ of the oxidized catalyst provides evidence that bare $Cu^{2+}$ isolated cations may also be involved in the SCR.

(2) At low temperature, that is, 523 K, the surface is mainly populated by reduced $Cu^+$ species, which indicates that the oxidation of these species is the rate-determining step of the process. In contrast, whatever the catalyst, at high temperature $[Cu-O-Cu]^{2+}$ is the main species which proves that the rate-determining step has shifted from oxidation to reduction.

(3) The different behaviors between the catalysts can be explained to a great extent by the redox properties of the materials. For instance, at low temperature, the catalyst which is the most easily oxidable, that is, Cu(0.16)Ba−FAU, is also the most active.

**Acknowledgment.** The calculations were carried out on the IBM SP4 computer of the CINES (Centre Informatique National de l'Enseignement Supérieur) in Montpellier (France). The authors thank Philippe Gonzales for technical help. Enrique Ayala-Villagomez is grateful to CONACYT (Mexico) for a scholarship.

## References and Notes

(1) Bosch, H.; Janssen, F. J. *Catal. Today* **1988**, *2*, 369. Janssen, F. J. In *Handbook of Heterogeneous Catalysis*; Ertl, G., Knözinger, H., Weitkamp, J., Eds.; Wiley-VCH: Weinheim, 1997; p 1633.

(2) Byrne, J. W.; Chen, J. M.; Speronello, B. K. *Catal. Today* **1992**, *13*, 33.

(3) Gry, P. *La Pollution Atmosphérique d'Origine Industrielle*. Presented at $NO_x$CONF, Paris, March 21−22, 2001; Session 8.

(4) Delahay, G.; Berthomieu, D.; Goursot, A.; Coq, B. In *Interfacial Applications in Environmental Engineering*; Keane, M. A., Ed.; Marcel Dekker: New York, 2002; p 1.

(5) Kieger, S.; Delahay, G.; Coq, B.; Neveu, B. *J. Catal.* **1999**, *183*, 267.

(6) Kieger, S.; Delahay, G.; Coq, B. *Appl. Catal., B* **2000**, *25*, 1.

(7) Delahay, G.; Ayala-Villagomez, E.; Ducéré, J. M.; Berthomieu, D.; Goursot, A.; Coq, B. *CHEMPHYSCHEM* **2002**, *3*, 686.

(8) Coq, B.; Delahay, G.; Fajula, F.; Kieger, S.; Neveu, B. *EU Pat.* 1999, 0914866 A.

(9) *Cerius2;* molecular modeling software for materials research; Accelrys, Biosym Technologies: San Diego, CA, 1993.

(10) Frisch, M. J.; G. W. T., Schlegel, H. B.; Scuseria, G. E.; Robb, M. A.; J. R. C.; Montgomery, J. A. Jr.; Vreven, T.; Kudin, K. N.; J. C. B.; Millam, J. M.; Iyengar, S. S.; Tomasi, J.; Barone, V.; B. M.; Cossi, M.; Scalmani, G.; Rega, N.; Petersson, G. A.; H. N.; M. Hada, M. Ehara, K. Toyota; R. Fukuda, J. H., M. Ishida, T. Nakajima, Y. Honda, O. Kitao; H. Nakai, M. K., X. Li, J. E. Knox, H. P. Hratchian, J. B. Cross; C. Adamo, J. J., R. Gomperts, R. E. Stratmann, O. Yazyev; A. J. Austin, R. C., C. Pomelli, J. W. Ochterski, P. Y. Ayala; K. Morokuma, G. A. V., P. Salvador, J. J. Dannenberg; V. G. Zakrzewski, S. D., A. D. Daniels, M. C. Strain; O. Farkas, D. K. M., A. D. Rabuck, K. Raghavachari; J. B. Foresman, J. V. O., Q. Cui, A. G. Baboul, S. Clifford; J. Cioslowski, B. B. S., G. Liu, A. Liashenko, P. Piskorz; I. Komaromi, R. L. M., D. J. Fox, T. Keith, M. A. Al-Laham; C. Y. Peng, A. N., M. Challacombe, P. M. W. Gill; B. Johnson, W. C., M. W. Wong, C. Gonzalez, and J. A. Pople, J. A. *Gaussian 03*; Revision B.03; Gaussian, Inc.: Pittsburgh, PA, 2003.

(11) Flannigen, E. M.; Khutami, H.; Szymanski, H. A. In *Molecular Sieve zeolite-I*; Gould, R. F., Ed.; Advances in Chemistry Series 101; American Chemical Society: Washington, DC, 1971; p 201.

(12) Valyon, J.; Hall, W. K. *J. Phys. Chem.* **1993**, *97*, 7054.

(13) Dalla Betta, R. A.; Garten, R. L.; Boudart, M. *J. Catal.* **1976**, *41*, 40.

(14) Komatsu, T.; Ogawa, T.; Yashima, T. *J. Phys. Chem.* **1995**, *99*, 13053.

(15) Naccache, C. M.; Ben Taarit, Y. *J. Catal.* **1971**, *22*, 171.

(16) Sárkány, J.; Sachtler, W. M. H. *Zeolites* **1994**, *14*, 7. Lei, G. D.; Adelman, B. J.; Sárkány, J.; Sachtler, W. M. H. *Appl. Catal., B* **1995**, *5*, 245. Sobalik, Z.; Tvarůžková, Z.; Wichterlová, B. *J. Phys. Chem. B* **1998**, *102*, 1077.

(17) Sobalik, Z.; Dědeček, J.; Ikonnikov, I.; Wichterlová, B. *Microporous Mesoporous Mater.* **1998**, *21*, 525.

(18) Sobalik, Z.; Šponer, J. E.; Tvarůžková, Z.; Vondrová, A.; Kuriyavar, S.; Wichterlová, B. *Stud. Surf. Sci. Catal.* **2001**, *135*, 136.

(19) Delahay, G.; Kieger, S.; Neveu, B.; Coq, B. *J. Chim. Phys.* **1999**, *96*, 443.

(20) Sárkány, J.; d'Itri, J. L.; Sachtler, W. M. H. *Catal. Lett.* **1992**, *16*, 241.

(21) Goodman, B. R.; Hass, K. C.; Schneider, W. F.; Adams, J. B. *J. Phys. Chem. B* **1999**, *103*, 10452.

(22) Hamada, H.; Matsubayashi, N.; Shimada, H.; Kintaichi, Y.; Ito, T.; Nishijima, A. *Catal. Lett.* **1990**, 189.

(23) Grünert, N. W. H.; Joyner, R. W.; Shapiro, E. S.; Siddiqui, M. R. H.; Baeva, G. N. *J. Phys. Chem*. **1994**, *98*, 10832.
(24) Goodman, B. R.; Schneider, W. F.; Hass, K. C.; Adams, J. B. *Catal. Lett.* **1999**, *56*, 183.
(25) Berthomieu, D.; Ducéré, J.-M.; Goursot, A. *J. Phys. Chem. B* **2002**, *106*, 7483.
(26) Berthomieu, D.; Krishnamurty, S.; Coq, B.; Delahay, G.; Goursot, A. *J. Phys. Chem. B* **2001**, *105*, 1149.
(27) Hadjivanov, K. I. *Catal. Rev.—Sci. Eng*. **2000**, *42*, 71.
(28) Centi, G.; Perathoner, S. *Appl. Catal., A* **1995**, *132*, 179.
(29) Williamson, W. B.; Lunsford, J. H. *J. Phys. Chem*. **1976**, *80*, 2664. Mizumoto, M.; Yamazoe, N.; Seiyama, T. *J. Catal*. **1979**, *59*, 319.
(30) Delahay, G.; Coq, B.; Kieger, S.; Neveu, B. *Catal. Today* **1999**, *54*, 431.
(31) Komatsu, T.; Nunokawa, M.; Moon, I. S.; Takahara, T.; Namba, S.; Yashima, T. *J. Catal.* **1994**, *148*, 427.
(32) Brandin, J. G. M.; Andersson, L. A. H.; Odenbrand, C. U. I. *Catal. Today* **1989**, *4*, 187.